International Journal of Basic and Applied Sciences, 6 (1) (2017) 7-16

International Journal of Basic and Applied Sciences

Website: www.sciencepubco.com/index.php/IJBAS
doi: 10.14419/ijbas.v6i1.6647
Research paper



Adsorptive removal of catechol and resorcinol by orange flavedo (citrus sinensis): mechanisms based on the flavedo components d-limonene, carotenoids, ascorbates, flavonoids and hydroxycinnamic acids

Kamgaing Théophile [1]*, Doungmo Giscard [1], Ngouoko Kouanang Jimmy Julio [1], Tchieno Melataguia Francis Merlin [1], Ketcha Joseph Mbadcam [2]

[1] *Laboratory of Noxious Chemistry and Environmental Engineering, University of Dschang P.O. BOX: 67 Dschang, Cameroon*
[2] *Department of Inorganic Chemistry, Faculty of Science, University of Yaoundé I, P.O. Box 812, Yaoundé-Cameroon*
**Corresponding author E-mail: theophile.kamgaing@univ-dschang.org*

Abstract

Orange flavedo and its adsorption behavior towards catechol (Ctc) and resorcinol (Res) were studied. Adsorption experiments were conducted in batch mode at room temperature. X-ray diffraction (XRD), Scanning electron microscopy (SEM), Energy-dispersive X-ray spectroscopy (EDX), Brunauer−Emmett−Teller (BET) and Fourier transform infrared (FTIR) data were used to characterize the biosorbent. The Effects of various parameters including equilibrium pH, sorbent dosage, initial adsorbate concentration and contact time were investigated. The optimum contact time and pH for the removal of Ctc and Res were 35 min and pH 2 respectively. The adsorption isotherms fitted well with Freundlich model, the adsorption of Ctc and Res being multilayer and the surface of orange flavedo heterogeneous; the pseudo-second order kinetic model better reflects the adsorption phenomena. An adsorption mechanism based on the molecules grafted to the surface of the orange flavedo is proposed in this study. 0.2 gram of the biosorbent was sufficient to completely eliminate 2.2 milligrams of resorcinol and catechol from solution. Therefore, non-modified orange flavedo is a promising candidate, as a low-cost biosorbent, for the removal of Ctc and Res from aqueous solution.

Keywords: *Orange Flavedo; Adsorption; Catechol; Resorcinol; Adsorption Mechanisms.*

1. Introduction

Orange is one of the most consumed fruits in the world. 50 million tons are produced annually, Brazil being leader with over 18 million tons. After extracting the juice, orange peels are discarded. Estimated at 25 million tons per year, the orange peels are a perfect example of lost resource. Yet, they contain more ascorbic acid (vitamin C) and more active compounds (D-limonene, hesperidin, naringin, auraptene ...) than the juice and the pulp [1]. The citrus peel consists of the white albedo which contains the primary vascular system of the fruit, the colored outer flavedo which contains oil glands and pigments, and the epidermal layer which contains stomatal guard cells and is covered by the cuticle [2], a thin "3 µm for citrus fruit" continuous polymer that plays a pivotal role in the growth and storage of citrus fruit [3,4]. Stomatal pores and flavedo components (ascorbates, flavonoids, terpenoids, pectines etc) give the orange peels interesting surface properties. The stomatal pores also act as a site for penetration of organisms and chemicals into the fruit. Many of these pores become plugged with wax but many remain functional [3]. In this study we focus on the external part of the orange peels (flavedo) whose cuticle is the main barrier through which exchanges are made between the orange and water, gases and various pollutants including Catechol (Ctc) and resorcinol (Res).

.

Ctc and Res are found in the effluents of industries such as textile, paper and pulp, steel, petrochemical, petroleum refinery, pharmaceutical, cosmetic, dye etc and in the wastewater of synthetic coal fuel conversion process [5], [6]. The toxicity of Ctc towards microorganisms, animals and human cell lines has been reported [7-9]. Although Ctc is more toxic than Res [7], [10], both are considered as the primary pollutants in wastewater due to their low biodegradability, high oxygen demand, and high toxicity [5], [9].
In this study, the orange flavedo is applied to the removal of Ctc and Res in solution. Before this, spectroscopic and micrographic analyzes of the biosorbent were made to offer an adsorption mechanism that takes into account the functional chemical groups of the outer orange peels.

2. Materials and method

2.1. Preparation and characterization of the biosorbent

2.1.1. Adsorbent from orange peel (flavedo)

Fresh oranges from Nigeria (improved variety) were purchased from Mokolo market in Yaoundé city, Cameroon, washed with running water to remove the soluble impurities, peeled with a sharp knife, ensuring that the flavedo was not harvested alongside the albedo. Peelings (flavedo), once washed and rinsed with distilled water were dried under the sun, then in an oven at 60 °C for

Copyright © 2017 Kamgaing Théophile et al. This is an open access article distributed under the Creative Commons Attribution License, which permits unrestricted use, distribution, and reproduction in any medium, provided the original work is properly cited.

48 h before being crushed in a grinding mill and sieved. Orange peels of particle size less than 250 µm designated EVACSO were stored in plastic bags for subsequent analyzes. The chemical treatment of EVACSO with sodium hydroxide, nitric acid, methanol and acetone leads to less satisfactory yields. For this reason, the biomaterial was used in its natural state to remove Ctc and Res in solution.

2.1.2. Characterization of orange flavedo (EVACSO)

2.1.2.1. Determination of pHpzc

The point of zero charge (pH_{pzc}) is the pH at which the adsorbent is neutral in aqueous suspension. It was determined following the procedure given by Lopez-Ramon [11].

2.1.2.2. BET analysis

The Brunauer−Emmett−Teller (BET) specific surface area of the samples was determined by nitrogen adsorption at 77 K with a Micromeritics instrument, Gemini Model 2380.

2.1.2.3. SEM analysis

Scanning Electron Microscopy (Phillips XL 30, Netherlands) images were taken to know the surface morphology of EVACSO.

2.1.2.4. EDX analysis

Energy dispersive X-ray spectroscopy (EDX) helped to determine the elementary composition of the orange flavedo.

2.1.2.5. XRD analysis

X-ray powder profiles were collected using a Bruker D5005 X-ray diffractometer equipped with sealed Cu-Kα radiation source (λ = 1.54184 Å).

2.1.2.6. FTIR analysis

Fourier Transform Infrared (FTIR) spectroscopy is a helpful tool in identifying the presence of certain functional groups on the surface of a solid. The biosorbent was analyzed using a FTIR Bruker Alpha-P spectrophotometer.

2.2. Preparation of Ctc and Res

Stock solutions of Ctc and Res (500 $mg.L^{-1}$) were obtained by dissolving known amounts of Ctc and Res in hydrogen peroxide-water mixture (1/5 v/v). Several dilutions were made later in the same conditions.

2.3. Optimization of Ctc and Res adsorption on EVACSO

The adsorption experiments were conducted in batch mode by mechanical agitation at room temperature. 50 mg of EVACSO of particle size less than 250µm were introduced into a flask containing 15 mL of Ctc or Res at the concentration 150 $mg.L^{-1}$. The mixture was stirred for 35 min and after filtration, Ctc and Res were analyzed using a UV/Vis spectrophotometer Jenway 6715, at the wavelengths 279 nm and 269 nm respectively. Similar assays were performed by varying the contact time, pH, adsorbent dosage and the initial concentrations of Ctc and Res. Adsorption percentage (%R) and amount (Q_E) adsorbed were obtained from equations (1) and (2) respectively.

$$\%R = \frac{(C_0 - C_E)100}{C_0} \quad (1)$$

$$Q_E = \frac{(C_0 - C_E)V}{m} \quad (2)$$

C_0 ($mg.L^{-1}$) and C_E ($mg.L^{-1}$) are respectively the initial concentration and the equilibrium concentration of Ctc and Res, m (mg) is the mass of the adsorbent and V (L) is the volume of the solution.

2.3.1. Effect of contact time

In ten bottles of 25 mL each were introduced 0.050 g of EVACSO and 15 mL of 150 $mg.L^{-1}$ sorbate. The mixtures were shaken at a constant speed and filtered at regular time intervals: 5-120 min. The filtrate was then analyzed by UV-Vis spectrophotometry to determine the residual concentration of Ctc and Res. The equilibrium time is obtained graphically by plotting quantity adsorbed at time t (Q_t) against time (t).

2.3.2. Effect of pH

The approach is the same as previously but at variable pH in the range from 2-11 and after a contact time of 35 min. The pH of the medium is adjusted using nitric acid 0.1M or sodium hydroxide 0.1M. The optimum pH is obtained graphically by plotting quantity adsorbed (Q_{ads}) against pH.

2.3.3. Effect of initial concentration

50 mg of EVACSO were added to various solutions of Ctc and Res (50 – 210 $mg.L^{-1}$), the pH of the medium adjusted to 2 for an optimal contact time of 35 min.

2.3.4. Effect of the absorbent dosage

The optimal dosage of EVACSO at a given concentration of Ctc or Res is obtained by keeping constant the previously optimized parameters and by varying the mass of EVACSO (0.06 – 0.18 g).

2.4. Kinetics adsorption studies

Kinetic studies were carried out at constant concentration of Ctc and Res (150 $mg.L^{-1}$) and constant mass of EVACSO (50 mg). The mixture was stirred vigorously at increasing time interval, and then filtered and the adsorbate residue determined. To fit experimental data, a number of kinetic models were used. These are:

2.4.1. Pseudo-first order kinetic model

The Lagergren pseudo-first order model [12] is the earliest known equation describing the adsorption rate based on the adsorption capacity. The differential equation is generally expressed a follows:

$$\frac{dQ}{dt} = K_1(Q_E - Q_t) \quad (3)$$

Q_E ($mg.g^{-1}$) and Q_t ($mg.g^{-1}$) being the adsorption capacity at equilibrium and at time t respectively and K_1 (min^{-1}) the rate constant of pseudo-first order adsorption. After integration, equation (3) becomes equation (4):

$$\ln(Q_E - Q_t) = \ln Q_E - K_1 t \quad (4)$$

2.4.2. Pseudo-second order kinetic model

The characteristic equation of this model [13] is given by equation (5):

$$\frac{dQ_t}{dt} = K_2(Q_E - Q_t)^2 \quad (5)$$

Better expressed as:

$$\frac{t}{Q_t} = \frac{1}{K_2 Q_E^2} + \frac{t}{Q_E} \quad (6)$$

K_2 being the rate constant for the pseudo-second order adsorption ($g.mg^{-1}.min^{-1}$).

2.4.3. The Elovich kinetic model

The Elovich kinetic equation is expressed as equation (7):

$$\frac{dQ_t}{dt} = \alpha \exp^{(\beta Q_t)} \quad (7)$$

Where α ($mg.g^{-1}.min^{-1}$) and β ($g.min^{-1}$) are the initial adsorption rate and the desorption constant respectively. Once integrated, equation (7) becomes equation (8):

$$Q_t = \frac{1}{\beta}\ln(\alpha\beta) + \frac{1}{\beta}\ln t \quad (8)$$

2.4.4. Intraparticle diffusion model

The intraparticle diffusion has often been regarded as the limiting step of most adsorption processes. The equation that better reflects the phenomenon is the following:

$$Q_t = K_d t^{1/2} + C \quad (9)$$

Where Q_t ($mg.g^{-1}$) and K_d are the instantaneous amount of adsorbate per unit gram of adsorbent and the diffusion constant respectively. C is a constant giving an idea about the thickness of the boundary layer.

2.5. Batch equilibrium experiments (adsorption experiments)

The adsorption isotherms derived from empirical models help to determine the type of interaction (chemisorption or physisorption) which leads to the adsorption of a molecule on the surface of a solid. Models commonly used are that of Langmuir, Freundlich and Temkin.

2.5.1. The Langmuir isotherm

The Langmuir isotherm model ensures a fixation of the adsorbate in a single layer on uniform sites and in a limited number of the adsorbent, without the possibility of transmigration of the adsorbate in the plane of the surface [14]. Equation (10) gives the linear form of the characteristic equation of this model:

$$\frac{C_E}{Q_E} = \frac{1}{Q_m K_L} + \frac{C_E}{Q_m} \quad (10)$$

Where Q_E ($mg.g^{-1}$) is the amount of adsorbate (Ctc or Res) adsorbed per unit mass of adsorbent (EVACSO), C_E ($mg.L^{-1}$) the equilibrium concentration of the adsorbate, Q_m ($mg.g^{-1}$) and K_L ($L.mg^{-1}$) are the monolayer adsorption capacity and the Langmuir adsorption constant respectively.

2.5.2. The freundlich isotherm

The Freundlich isotherm, based on adsorption on a heterogeneous surface [15] is characterized by the following equation

$$\ln Q_E = \ln K_F + \frac{1}{n}\ln C_E \quad (11)$$

Where K_F is a constant related to the adsorption capacity and $\frac{1}{n}$ is an empirical parameter related to the adsorption intensity, which varies with the heterogeneity of the material [16]. If the value of $\frac{1}{n}$ is below one, it indicates a normal adsorption.

2.5.3. The temkin isotherm

The following equation is a fundamental characteristic of the Temkin model [17]:

$$Q_E = Q_m \frac{RT}{\Delta Q}\ln K_T C_E \quad (12)$$

Where Q_E is the amount adsorbed at equilibrium, K_T the equilibrium constant and ΔQ the heat of adsorption. The linear form of this equation is:

$$Q_E = Q_m \frac{RT}{\Delta Q}\ln K_T + Q_m \frac{RT}{\Delta Q}\ln C_E \quad (13)$$

By plotting $Q_E = f(\ln C_E)$, one obtains a straight line whose slope and intercept make it possible to determine the heat of adsorption ΔQ and the equilibrium constant K_T.

3. Results and discussion

3.1. Characterization of the adsorbent material (EVACSO)

3.1.1. The point of zero charge (pHpzc)

The pH of zero charge EVACSO is 4.72. Thus, when the pH of the medium is less than 4.72, the surface charge of the biomaterial is generally positive. Under these conditions, the EVACSO-Ctc and EVACSO-Res interactions are attractive through hydrogen bond formation or covalent bond formation.
When the pH is higher than 4.72, the surface charge is negative and interactions become repulsive.

3.1.2. BET analysis

Table 1 indicated the BET surface area of some natural biosorbents. It should be noted that the surface area of orange flavedo ($0.72\ m^2.g^{-1}$) is the same as that of the sawdust, but significantly higher than that of the rice husk.

Table 1: Specific Surface Area of Some Natural Sorbents

Sorbent	BET surface area ($m^2.g^{-1}$)	Reference
Peat	1.02	[18]
Sawdust	0.72	[18]
Bagasse	1.67	[18]
Rice husk	0.24	[18]
Orange flavedo	0.72	This study

3.1.3. SEM analysis

The morphology of EVACSO was characterized using scanning electron microscopy (SEM). Fig. 1 shows the SEM micrograph of EVACSO, revealing the irregular and porous surface of the sample used. This confirms similar observations by Arami et al. [19] and Mafra et al. [20].

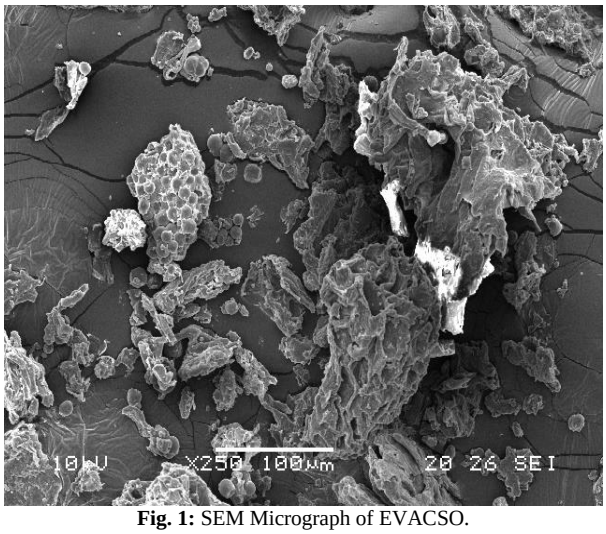


Fig. 1: SEM Micrograph of EVACSO.

3.1.4. EDX analysis

The bulk composition of EVACSO was investigated by energy dispersive X-ray (EDX) measurements. The EDX spectrum obtained is shown in Fig. 2. The atomic and weight percentages of the agricultural waste material are summarized in table 2, with carbon and oxygen being the most abundant elements by weight.

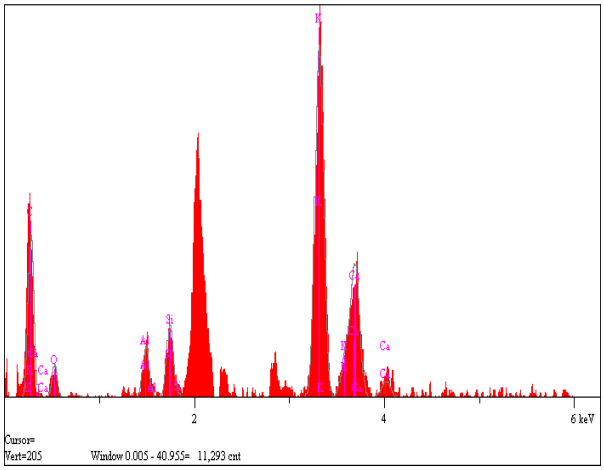


Fig. 2: EDX Spectrum of EVACSO.

Table 2: Elemental Analysis of EVACSO

Element	wt%	At%
K	12.867	26.834
O	20.585	17.568
C	55.788	35.741
Al	2.035	2.928
Si	2.693	4.034
Ca	6.032	12.895

3.1.5. XRD analysis

EVACSO was further characterized by powder X-ray diffraction (XRD). The diffractogram obtained is depicted by Fig. 3. The diffused diffraction peaks around 20° corresponds to the amorphous structures of carbon [21]. The absence of any ordered crystalline structure is confirmed.

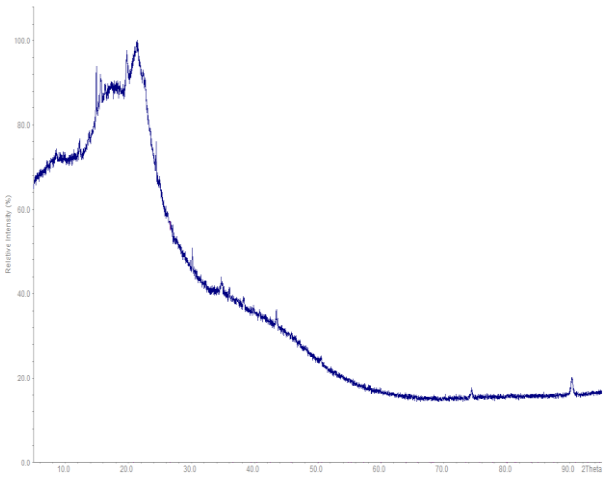


Fig. 3: XRD Spectrum of EVACSO.

3.1.6. FTIR analysis

Fourier transform infrared (FTIR) spectroscopy was used to identify the functional groups present in EVACSO. The FTIR spectrum obtained in the 4000-400 cm^{-1} spectral region is shown in Fig. 4 and the band assignments summarized in table 3. The broad band at the high energy region centered around 3293.32 cm^{-1} is assigned to O-H stretching vibrations (flavanone aglycones and their respective glycosides, vitamin C, hydroxycinnamic acids). The peak at 2923.33 cm^{-1} corresponds to the C-H stretching of methyl (limonene...) and methylene moieties (aglycones and glycosides) while the band at 1736.75 cm^{-1} can be assigned to C=O stretching vibrations (flavanone aglycones and glycosides, vitamin C, hydroxycinnamic acids). The adsorption bands around 529 cm^{-1} can be attributed to Si-O bending vibrations.

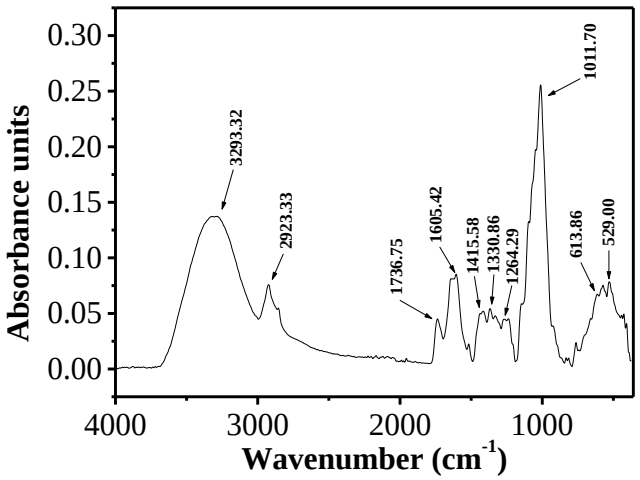


Fig. 4: FTIR Spectrum of EVACSO.

Table 3: Characteristic Infrared Bands of EVACSO

Wavenumber (cm^{-1})	Assignment
3293.32	νO-H
2923.33	νC-H
1736.75	νC=O
1605.42	νC=C
1415.58	δ_{as}C-H
1367.52	δ_{s}C-H
1330.86	δ CH_2
1264.29	νAryl-OH
1011.70	νC-O
613.86	δ C=O
529.00	δ Si-O

ν: stretching, δ: bending, δ_{as}: asymmetrical bending, δ_{s}: symmetrical bending

3.2. Adsorption experiments

3.2.1. Effect of contact time

The adsorption of Res and Ctc occurs in two steps (Fig. 5). The first step which is rapid occurs in less than 10 min and the quantity adsorbed for both was 15 mg.g^{-1}. Indeed, the adsorbent adsorption sites are uncongested at this stage: no obstacles that may hinder the diffusion of molecules Ctc and Res. After 35 min, the second step occurs with a maximum adsorbed quantity of 25 mg.g^{-1}. At this stage, the repulsive forces between the adsorbed molecules and molecules in solution become important. This phenomenon has been described by many authors [22], [23].

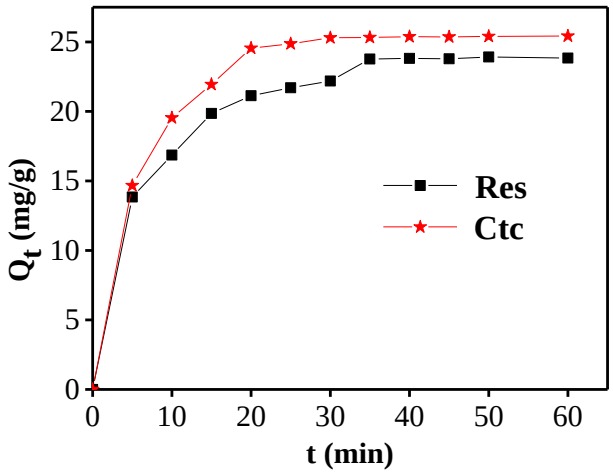


Fig. 5: Effect of the Contact Time on the Adsorption of Res and Ctc by EVACSO. Test Conditions: 15 Ml of 150 Mg.L^{-1}analyte, 50 Mg of Adsorbent, Stirring Speed 125 Rev/Min, Room Temperature.

3.2.2. Effect of pH on Ctc and Res adsorption

The pH is an important parameter in the adsorption because it acts both on the surface charge of the adsorbent and on the adsorption medium; it significantly influences the interactions (repulsive/attractive) that take place between adsorbate and adsorbent, and between adsorbate molecules [24]. It is at pH 2 (very acidic pH) that the adsorption of Ctc and Res is optimal (Fig. 6). Indeed, when the pH increases, while the adsorbent surface charge becomes negative (pH > pH_{ZPC}), Ctc and Res become phenolates (catecholate, resorcinolate). Electrostatic repulsion between adsorbent and adsorbate then become paramount.

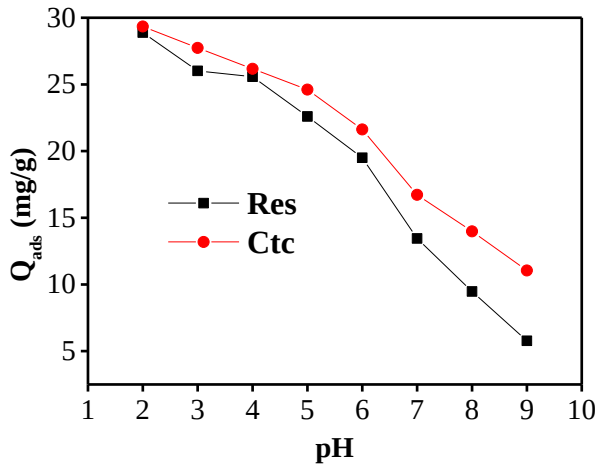


Fig. 6: Effect of Ph on the Adsorption of Res and Ctc by EVACSO. Experimental Conditions: 15 Ml of 150 Mg.L^{-1} Analyte, 50 Mg of Adsorbent, Stirring Speed 125 Rev/Min, Contact Time 35 Min, Room Temperature.

3.2.3. Effect of adsorbent dosage

At a given concentration of analyte, the adsorption efficiency increases with the adsorbent dosage (Fig. 7). The more the mass of adsorbent increases, the more the binding sites of the adsorbate become important, and the best is adsorption efficiency. However, 100 mg of EVACSO are enough to completely eliminate the Res in solution. It takes more (160 mg) to adsorb catechol at about 93%. Fig.7 shows that below 60 mg of adsorbent added, Ctc is more adsorbed than Res but above, Res is more adsorbed than Ctc.

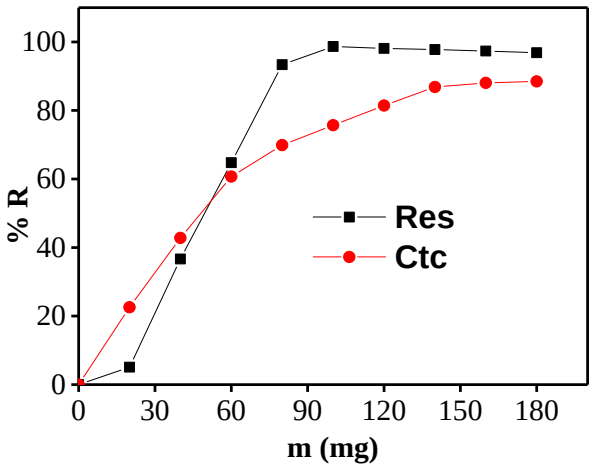


Fig.7: Effect of the Adsorbent Dosage on the Adsorption of Res and Ctc by EVACSO. Experimental Conditions: 15 Ml Of 150 Mg.L^{-1} Analyte, Ph 2, Stirring Speed 125 Rev/Min, Contact Time 35 Min, Room Temperature.

3.2.4. Effect of initial adsorbate concentration

The adsorption of Ctc and Res on orange flavedo increases with the concentration (Fig. 8). In the range of concentrations studied, the maximum adsorption capacity of the biosorbent is 27.5 mg.g^{-1} for Ctc and 34.4 mg.g^{-1} for Res.

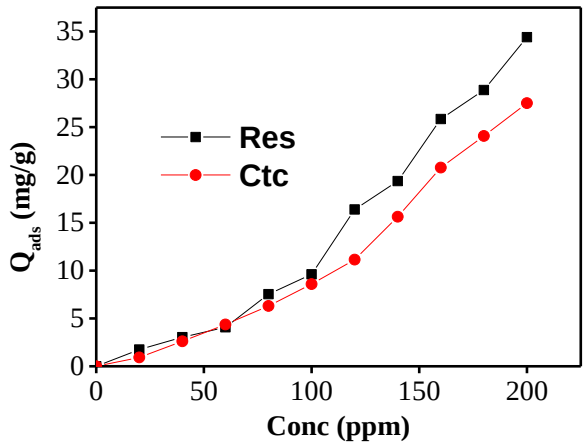


Fig.8: Effect of the Initial Concentration on the Adsorption of Res and Ctc by EVACSO. Experimental Conditions: 15 Ml of Analyte, 50 Mg of Adsorbent, Ph 2, Stirring Speed 125 Rev/Min, Contact Time 35 Min, Room Temperature.

3.2.5. Adsorption isotherms

Linear plots of the models of Langmuir, Freundlich and Temkin are represented in Figs. 9-11. The values of correlation coefficients are significant for all models studied (R^2 > 0.9, table 4). However, the Freundlich isotherm (R^2 = 0.993) and that of Langmuir (R^2 = 0.977) better reveal the adsorption phenomena of Res on the surface of the orange flavedo (EVACSO). This is also the case with Ctc (Langmuir, R^2 = 0.997; Freundlich, R^2 = 0.9896). However the Freundlich model is to be consider as Langmuir Q_m values (16 mg.g^{-1}for Ctc and 4.47 mg.g^{-1}for Res) are well below the experimental values (34.4 mg.g^{-1} for Res and 27.5mg.g^{-1} for Ctc). On the other hand, the n value of Freundlich is less than 1 in both cases, indicating the physisorption of Ctc and Res. Since the experimental data better obey the Freundlich isotherm and adsorption being physisorption type, it is probable that the adsorption of

Ctc and Res is multilayer and the surface of flavedo heterogeneous. Other authors have argued in the same vein with orange peels applied to chrome removal [25].

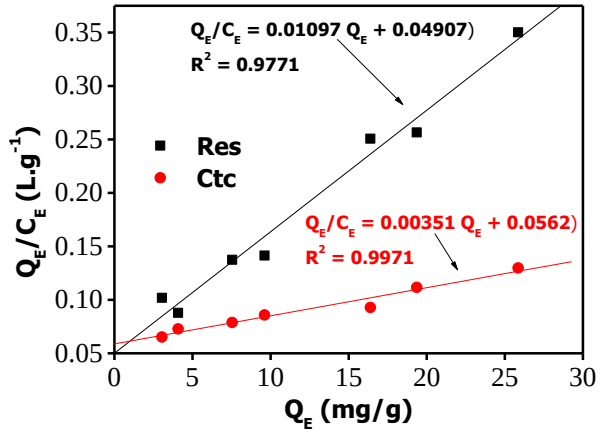


Fig. 9: Langmuir Isotherm Sorption Model. Experimental Conditions: 15 Ml of (60-180 Mg.L^{-1}) Analyte, 50 Mg of Adsorbent, Ph 2, Stirring Speed 125 Rev/Min, Contact Time 35 Min, Room Temperature.

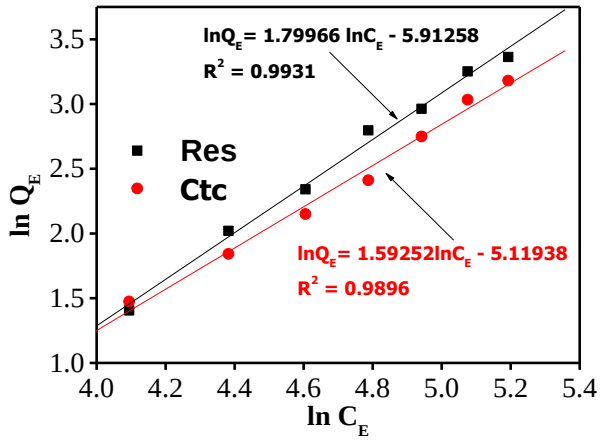


Fig. 10: Freundlich Isotherm Sorption Model. Experimental Conditions: 15 Ml of (60-180 Mg.L^{-1}) Analyte, 50 Mg of Adsorbent, Ph 2, Stirring Speed 125 Rev/Min, Contact Time 35 Min, Room Temperature.

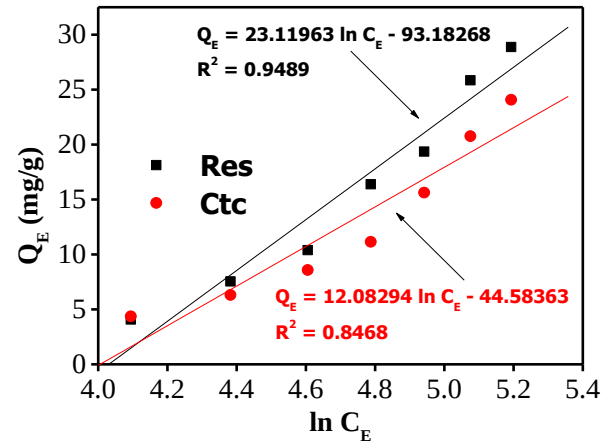


Fig. 11: Temkin Isotherm Sorption Model. Experimental Conditions: 15 Ml of (60-180 Mg.L^{-1}) Analyte, 50 Mg of Adsorbent, Ph 2, Stirring Speed 125 Rev/Min, Contact Time 35 Min, Room Temperature.

Table 4: Langmuir, Freundlich and Temkin Constants and Adsorption Parameters

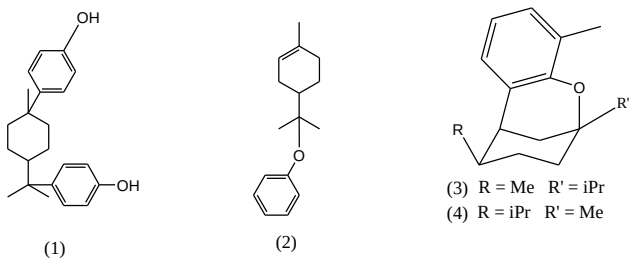
Adsorbent		EVACSO	
Isotherm	Parameters	Res	Ctc
Langmuir isotherm	K_L (L/mg)	0,01097	0,00361
	Q_m (mg/g)	4,473	16,011
	R_L	0,3629	0,64
	R^2	0,9771	0,9971
Freundlich isotherm	K_F (L/mg)	0,00271	0,006
	1/n	1,79966	1,59252
	R^2	0,9931	0,9896
Temkin isotherm	K_T (L/g)	0,0178	0,250
	ΔQ (J/mol)	107,163	205.047
	R^2	0,9489	0,8468

3.2.6. Adsorption mechanism

It appears that several barriers are erected during the development of orange: cuticle (consisting of matrix and waxes) the outermost part of the flavedo is the primary barrier; then the epidermal layer that contains the stomatal guard cells (penetration sites of chemicals and so forth), then the albedo, and finally the pulp that contains the juice. Exchanges take place by crossing all these barriers. In our case, Ctc and Res cross the barrier erected by the flavedo cuticule, weakened in very acidic medium (pH = 2). These phenols are then adsorbed in the pores of the stomata. Their chemisorption is facilitated by the hydrogen and covalent bonds formation with the molecules of flavedo which are phenolics (e.g. flavonone glycosides, hydroxycinnamic acids), ascorbates (vitamine C), carotenoids [26-28], flavonoids Naringin and hesperidin [29] and D-limonene, a major constituent in several citrus oils (orange, lemon, mandarin, lime, and grapefruit) [30]. The adsorption of catechol and resorcinol could not be done without the contribution of these surface molecules, adsorption which is usually done in three steps: the transfer of the adsorbate to the outer surface of the adsorbent (diffusion layer), the migration of the adsorbate from the outer surface to the inner surface of the adsorbent, and the sorption of the adsorbate to the internal surface of the pores of the adsorbent. The mechanisms we propose below reflect the molecules on the surface of flavedo.

3.2.6.1. Mechanism involving limonene, main sensitizer of orange peels

The outer layer of orange peel consists of numerous oil-containing cells from which an oil of limonene, other terpenes, linalool, and a resinous residue can be expressed [31]. The terpene, limonene, is probably the principal sensitizer of orange peels. Its chemistry is vast. Its action on the acids, bases, alcohols and other reagents is described [32]. The reaction of limonene with phenols dates from 1922 [33], and the products have been patented as resins and lacquers. Products derived from this reaction could arise either by aromatic substitution (Fig. 12), formation of phenol ether [34], aromatic substitution followed by epoxidation if one refers to o-cresol [35], further reaction giving polymers [36-37].



(1) (2)

Fig. 12: Terpene-Phenol Monomers (Aromatic Substitution (1), Formation of Phenol Ether (2), Aromatic Substitution **followed by** Epoxidation (3) **and** (4).

3.2.6.1.1. Probable adsorption mechanism of Ctc and Res involving limonene

Non-activated orange flavedo has the advantage of keeping all functional groups present at its surface including limonene. The action of acids on this terpene leads to a carbocation [34] which rearranges as shown in Fig. 13. With this carbocation formed, the attractive electrostatic forces between adsorbent-adsorbate are prevailing. At this stage and by similarity to the phenol [34], there would be aromatic substitution of Ctc/Res (6) and even limonene-phenol ether formation (5) (Fig. 13). By analogy with o-cresol [37] the compounds (7) and (8) are possible. One can also think of the condensation of a hydroxy phenol (Ctc/Res) with 2 limonene molecules (9). It appears that limonene is involved in the chemisorption process of Ctc and Res by covalent bond formation (C-C and C-O bonds).

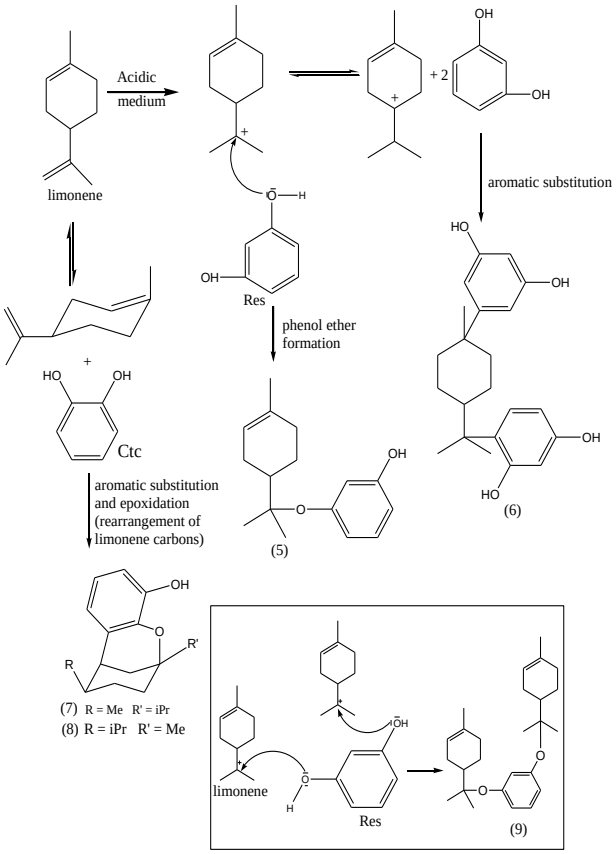


Fig. 13: Likely Reactions of Limonene on Ctc and Res.

3.2.6.2. Mechanism involving flavedo molecules having an OH group (vitamin C, phenolic compounds, flavonoids, hydroxycinnamic acid): hydrogen bond formation

The common point of flavonoids, hydroxycinnamic acids and ascorbic acid (vitamin C) contained in orange flavedo is that they all have hydroxylated groups in impressive numbers (Fig. 14). These form hydrogen bonds with the hydroxyl groups of Ctc and Res (Fig. 15).

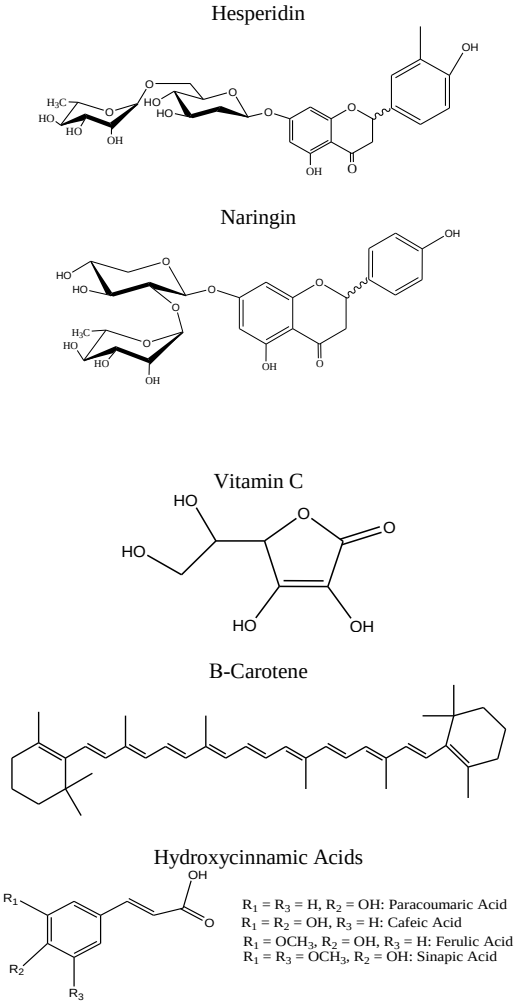
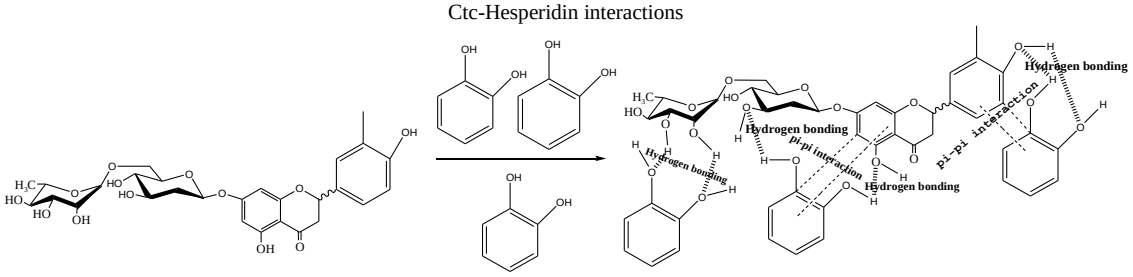


Fig. 14: Main Flavedo Components.

3.2.6.3. Mechanism involving the electron rich constituents of flavedo (carotenoids, flavonoids, hydroxycinnamic acids): π-π interactions.

Because Res and Ctc have benzene rings, it could be speculated that the main intermolecular force between these two molecules and the molecules of flavedo (flavonoids such as naringin and hesperidin, carotenoids like β-Carotene, ascorbates as vitamin C, and hydroxycinnamic acids) should be the π–π interaction (Fig. 15). The π electrons of benzene ring of Res and Ctc interact with C=C double bonds or the π electrons of benzene rings of flavedo molecules by means of π–π electron coupling. Jing et al. [38] thought the same thing about the adsorption of bisphenol A by graphene.



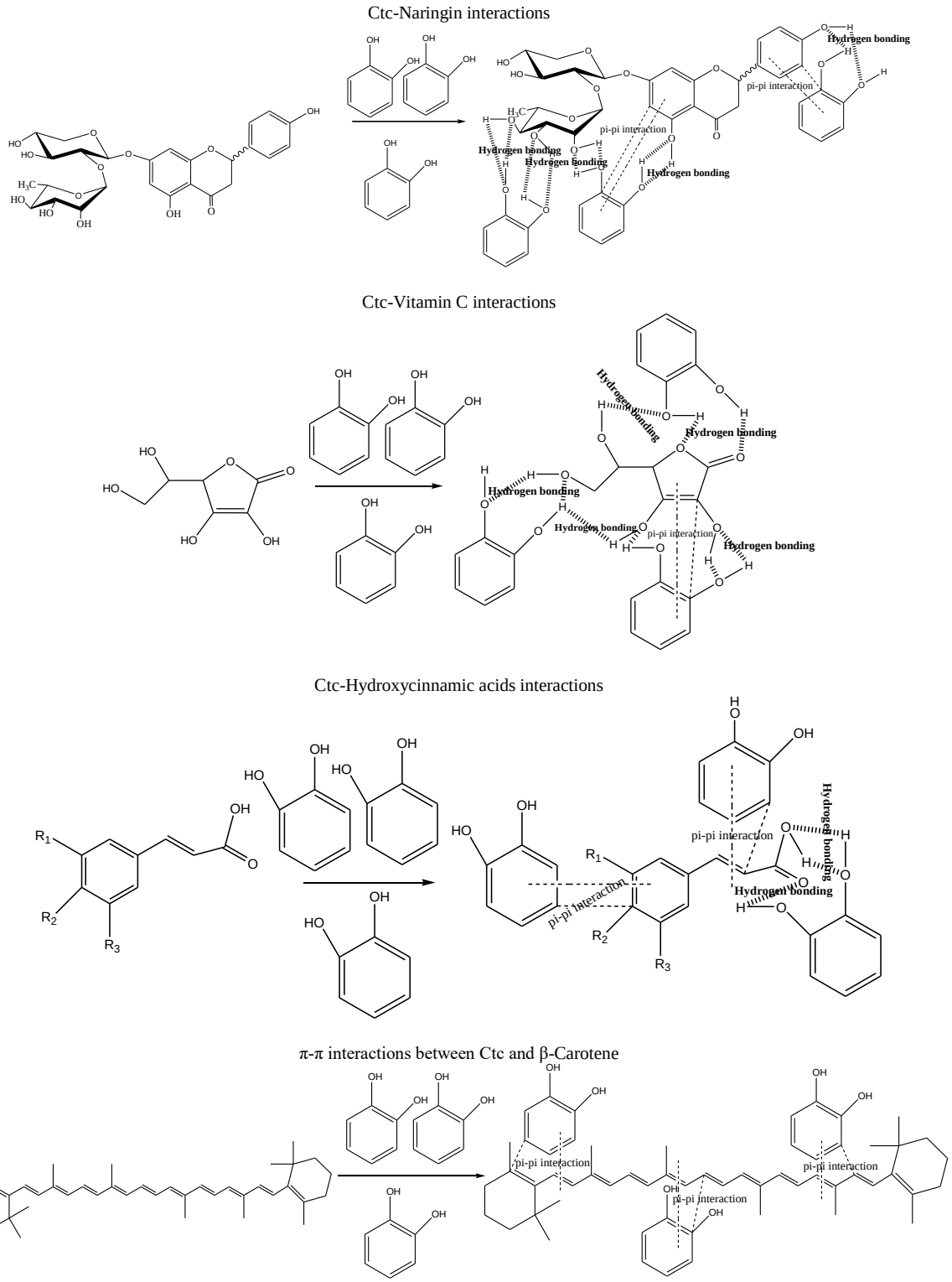


Fig. 15: Schematic of Hydrogen Bonding and Π-Π Interactions between Ctc and Flavedo Components.

Thus, we can expect that tree kinds of adsorbent−adsorbate interactions might be responsible for the adsorption of Ctc and Res on orange flavedo. One of the tree interactions is the π–π interaction between the benzene rings of Ctc/ Res and the flavedo molecules. The other is the attractive electrostatic interactions involving D-limonene in acidic medium. The last but not the least is hydrogen bonding between the oxygen containing groups contained in both Ctc/Res and flavedo.

3.2.7. Kinetic modeling of Ctc and Res adsorption

Four kinetic models involved in this study are summarized in Figs. 16-19. Table 5 shows the values of the corresponding kinetic parameters. The pseudo-second order kinetic model perfectly describes the adsorption of Ctc on EVACSO (R^2 = 0.9980 and Q_E = 27.2 mg.g^{-1}), very close to the experimental value (25.3 mg.g^{-1}). It is also the case of resorcinol (R^2 = 0.9985) although showing a low Q_E value (5.05 mg.g^{-1}) compared to the experimental value (23.8 mg.g^{-1}). The Elovich kinetic model (R^2 = 0.96) provides for Res an adsorption coefficient significantly higher (α = 24.743 mg.g^{-1}.min^{-1}) than the desorption coefficient (β = 0.02322 mg.g^{-1}.min^{-1}), indicating an attractive interaction between adsorbent and adsorbate.

It should be noted that the factor which limits the adsorption of Res is essentially the intraparticle diffusion, which is not the case of Ctc (Fig. 19). All the above considerations are in favor of a chemisorption of Res and Ctc in the inner surface of orange flavedo [13].

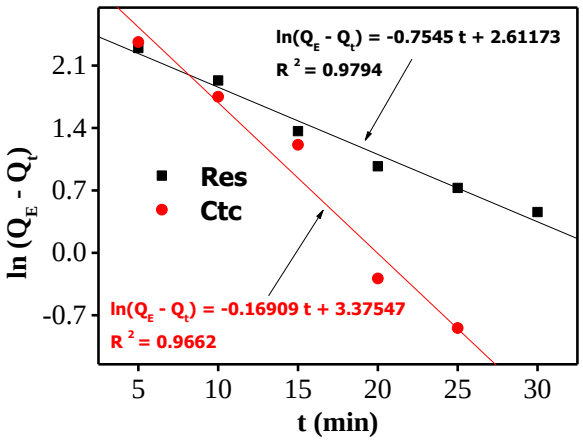


Fig. 16: Linearized Pseudo-First Order Plots.

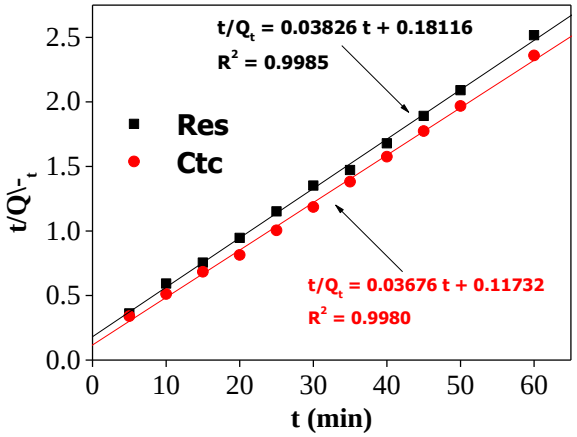


Fig. 17: Linearized Pseudo-Second Order Plots.

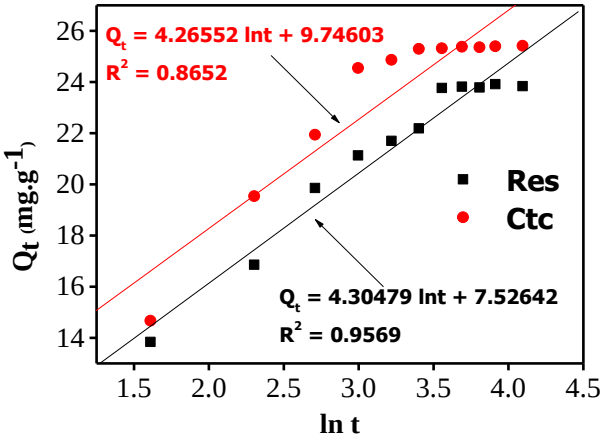


Fig. 18: Linearized Elovich Model Plots.

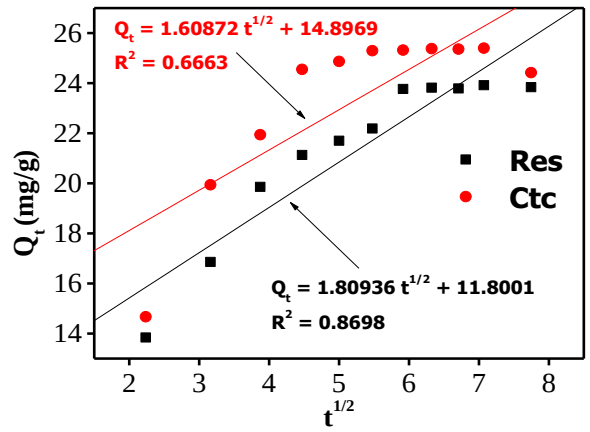


Fig. 19: Linearized Intraparticle Diffusion Model Plots.

Table 5: Kinetic Constants and Parameters of Four Adsorption Kinetic Models Involved in the Sorption of Ctc and Res Using EVACSO.

Adsorbent		EVACSO	
Kinetic models	Parameters	Res	Ctc
Pseudo-first order model	K_1 (min^{-1})	0.7541	0.16909
	Q_E ($mg.g^{-1}$)	13.62	29.24
	R^2	0.9794	0.9662
Pseudo-second order model	K_2 ($g.min^{-1}.mg^{-1}$)	1.0165	0.0115
	Q_E ($mg.g^{-1}$)	5.038	27.20
	R^2	0.9985	0.9980
	h ($mg.min^{-1}.g^{-1}$)	25.80	8.524
Elovich kinetic model	α ($mg.g^{-1}.min^{-1}$)	24.743	41.905
	β ($g.mg^{-1}$)	0.02322	0.2344
	R^2	0.9569	0.8652
Intraparticle diffusion model	K_d ($mg.g^{-1}.min^{-1/2}$)	1.8009	1.60872
	C_1 (mg)	11.8001	14.8969
	R^2	0.8698	0.6663

4. Conclusion

Orange peels, a major source of nutrient-rich residues also have important surface properties. In this study it is shown that they can be applied to the removal of catechol and resorcinol in solution. Surface molecules responsible for the adsorption of the two phenols are mainly limonene, carotenoids, flavonoids and hydroxycinnamic acids. They are responsible for the sorption of catechol and resorcinol by formation of hydrogen bonds and π- π interactions, and by covalent bond formation with the limonene. The adsorption is multilayer and the surface of flavedo heterogeneous. The kinetics are second order. The intraparticle diffusion is the limiting factor for the adsorption of resorcinol, which is not the case for catechol where other factors, in addition to the internal diffusion are to be considered. These results revealed that orange flavedo could be used as alternative low cost biosorbent for catechol and resorcinol removal from aqueous solution.

Acknowledgements

We thank the Ministry of Higher Education of Cameroon for the special premium paid quarterly to Lecturers, and MIPROMALO-Cameroon for his contribution to the analysis of materials.

References

[1] Hakim, I.A., Harris, R.B. (2001). Joint effects of citrus peel use and black tea intake on the risk of squamous cell carcinoma of the skin, Dermatology, 1:3. https://doi.org/10.1186/1471-5945-1-3.

[2] Albrigo, G. (1986). Peel morphology and fruit blemishes. Citrus Flowering, fruit set and development. Gainesville, University of Florida, 73-80.

[3] Petracek, P.D. (1997). Peel morphology and fruit blemishes. Citrus Flowering and Fruiting Short Course, CREC, Lake Alfred, 18-118.

[4] Agusti, M.; Zaragoza, S.; Bleiholder, H.; Buhr, L.; Hack, H.; Klose, R.; Stauss, R. (1997). Adaptation of the BBCH scale for the description of citrus fruits phenological stages, Fruits, 52, 287-295.

[5] Phutdhawong, W.; Chowwanapoonpohn, S.; Buddhasukh, D. (2000). Electrocoagulation and subsequent recovery of phenolic compounds, *Analytical Sciences*, 16, 1083–1084. https://doi.org/10.2116/analsci.16.1083.

[6] Schweigert, N.; Zehnder, A.J.B.; Eggen, R.I.L. (2001). Chemical properties of catechols and their molecular modes of toxic action in cells, from microorganisms to mammals, *Environmental Microbiology*, 3, 81–91. https://doi.org/10.1046/j.1462-2920.2001.00176.x.

[7] Raff, R.; Ettling, B.V. (1966). Hydroquinone, resorcinol and pyrocatechol, in: Kirk RE, Othmer D.F. (Eds.), Encyclopedia of Chemical Technology, Wiley, New York, 462–492.

[8] Steiman, R.R; Seigle-Murandi, F.; Chritov, L.P. (1999). Growth of 1044 strains and species of fungi on 7 phenolic lignin model compounds, *Chemosphere*, 38, 2549–2559. https://doi.org/10.1016/S0045-6535(98)00462-7.

[9] Van Duursen, M.B.M.; Sanderson, J.T.; De Jong, P.C.; Kraaij, M.; Van den Berg, M. (2004). Phytochemicals inhibit catechol-o-methyl transferase activity in cytosolic fractions from healthy human mammary tissues: implications for catechol estrogen-induced

DNA damage, *Toxicological Sciences*, 81, 316–324. https://doi.org/10.1093/toxsci/kfh216.
[10] Prager, J.C. (1996). Environmental Contaminant Reference Data book Volume 2, Van Nostrand Reinhold, New York, p. 560.
[11] Lopez-Ramon, M.V.; Stoeckli, F.; Moreno-Castilla, C.; Carrasco-Marin, F. (1999). On the characterization of acidic and basic surface sites on carbons by various techniques. *Carbon*, 37, 1215-1221. https://doi.org/10.1016/S0008-6223(98)00317-0.
[12] Lagergren, S. (1898). Zur theorie der sogenannten adsorption geloster stoffe, Kungliga Svenska Veten skapsakademiens, *Handlingar*, 24 (4), 1-39.
[13] Ho, Y.S. (2006). Review of second-order models for adsorption systems, *Journal of Hazardous Materials*, B136, 681-689. https://doi.org/10.1016/j.jhazmat.2005.12.043.
[14] Langmuir, I. (1918). The adsorption of gases on plane surfaces of glass, mica, and platinum. *Journal of the American Chemical Society*, 40, 1361-1403. https://doi.org/10.1021/ja02242a004.
[15] Freundlich, H. (1906). Over the adsorption in the solution. *Journal of Physical Chemistry*, 57, 385-470.
[16] Bourdais, E.; Fytianosand, F.; Bozani, E. (2002). Sorption Description isotherms of Dyes from aqueous solutions and Waste Waters with Different Sorbent materials, *Global Nest: the Int. J.*, 4, 75-83.
[17] Tempkin, M.I.; Pyzhev, V. (1940). Kinetics of ammonia synthesis on promoted iron catalyst. *Acta Physicochimica USSR*, *12*, 327–356.
[18] Yanbo, Z.; Ping, L.; Jun, L. (2012). Application of natural biosorbent and modified peat for Bisphenol A removal from aqueous solutions, *Carbohydrate Polymers*, 88, 502-508. https://doi.org/10.1016/j.carbpol.2011.12.034.
[19] Arami, M.; Limaee, N.Y.; Mahmoodi, N.M.; Tabrizi, N.S. (2005). Removal of dyes from colored textile wastewater by orange peel adsorbent: Equilibrium and kinetic studies, *Journal of Colloid and Interface Science*, 288, 371–376. https://doi.org/10.1016/j.jcis.2005.03.020.
[20] Mafra, M.R.; Igarashi-Mafra, L.; Zuim, D.R.; Vasques, É.C.; Ferreira, M.A. (2013). Adsorption of remazol brilliant blue on an orange peel adsorbent. *Brazilian Journal of Chemical Engineering*, 30, 657–665. https://doi.org/10.1590/S0104-66322013000300022.
[21] Guan, Q.; Xiong, W.; Zhou, L.; Liu, S. (2016). Facile synthesis of nitrogen-doped porous carbon-gold hybrid nanocomposite for mercury (II) ion electrochemical determination, *Electroanalysis*, 28, 133–139. https://doi.org/10.1002/elan.201500481.
[22] Kumar, A.; Kumar, S.; Kumar, S. (2003). Adsorption of resorcinol and catechol on activated carbon: equilibrium and kinetics. *Carbon*, 41, 3015–3025 https://doi.org/10.1016/S0008-6223(03)00431-7.
[23] Mohamed, F.S.; Khater, W.A.; Mostafa, M.R. (2006). Characterization and phenols sorptive properties of carbons activated by sulphuric acid, *Chemical Engineering Journal*, 116, 47–52.
[24] Moreno-Castilla, C. (2004). Adsorption of organic molecules from aqueous solutions on carbon materials, *Carbon*, 42, 83–94. https://doi.org/10.1016/j.carbon.2003.09.022.
[25] Fabian, A.U.; Aloysius, A.P.; Abiola, V.I. (2014). Thermodynamic Properties of Chromium (III) Ion Adsorption by Sweet Orange (*Citrus sinensis*) Peels, *American Journal of Analytical Chemistry*, 5, 666-673. https://doi.org/10.4236/ajac.2014.510074.
[26] Marchand, L. (2002). Cancer preventive effects of flavonoids-A review, *Biomedicine & Pharmacotherapy*, 56, 296–301. https://doi.org/10.1016/S0753-3322(02)00186-5.
[27] Halliwell, B. (1996). Antioxidants in human health and disease, *Annual Review of Nutrition*, 16, 33-50. https://doi.org/10.1146/annurev.nu.16.070196.000341.
[28] Rao, A.V.; Rao, L.G. (2007). Carotenoids and human health, *Pharmacological Research*, 55, 207–216. https://doi.org/10.1016/j.phrs.2007.01.012.
[29] Escobedo-Avellaneda, Z.; Gutierrez-Uribe, J.; Valdez-Fragoso, A.; Torres, J.A.; Welti-Chanes, J. (2014). Phytochemicals and antioxidant activity of juice, flavedo, albedo and comminuted orange, *Journal of Functional Foods*, 6, 470–481. https://doi.org/10.1016/j.jff.2013.11.013.
[30] Sun, J. (2007). D-Limonene: Safety and Clinical Applications, *Alternative Medicine Review*, 12, 259-264.
[31] Mondello, L.; Casilli, A.; Tranchida, P.Q. ; Dugo, P.; Dugo, G. (2005). Comprehensive two-dimensional GC for the analysis of *Citrus* essential oils, *Flavour and Fragrance Journal*, 20, 136-140. https://doi.org/10.1002/ffj.1506.
[32] Thomas, A.F.; Bessiere, Y. (1998). Limonene, *Natural Product Reports*, 291-309.
[33] Wuyts, H. Br. P. 204754, June 29, 1922 *Cheni. Zenrralbl.*, 1923, IV, 951.
[34] Hultzsch, K. (1938). *Angew. Cliem*, 51, 920. https://doi.org/10.1002/ange.19380515203.
[35] Kuzakov, E.V.; Schmidt, E.N. (2000). Synthesis of terpenophenols via direct alkylation of phenols by terpenes, *Chemistry of Natural compounds*, 36, 245-257. https://doi.org/10.1007/BF02238328.
[36] Remmelsburg, A.L.V. (1949). Hercules Powder Co., U.S. P. 2471455, May 31, *Chem. Ahstr*., 43, 6237.
[37] Fink, J.K. (2013). Reactive polymers fundamentals and applications. A concise Guide to industrial polymers, 2nd edition, Elsevier, 524 pp.
[38] Jing, X.; Li, W.; Zhu, Y. (2012). Decontamination of bisphenol A from aqueous solution by graphene adsorption, *Langmuir*, 28, 8418−8425. https://doi.org/10.1021/la301476p.